

# Magnetic Tunnel Junctions for Spintronic Memories and Beyond

Shoji Ikeda, Jun Hayakawa, Young Min Lee, Fumihiro Matsukura, Yuzo Ohno, Takahiro Hanyu, *Member, IEEE*, and Hideo Ohno, *Member, IEEE*

(Invited Paper)

**Abstract**—In this paper, recent developments in magnetic tunnel junctions (MTJs) are reported with their potential impacts on integrated circuits. MTJs consist of two metal ferromagnets separated by a thin insulator and exhibit two resistances, low ( $R_P$ ) or high ( $R_{AP}$ ), depending on the relative direction of ferromagnet magnetizations, parallel (P) or antiparallel (AP), respectively. Tunnel magnetoresistance (TMR) ratios, defined as  $(R_{AP} - R_P)/R_P$  as high as 361%, have been obtained in MTJs with  $\text{Co}_{40}\text{Fe}_{40}\text{B}_{20}$  fixed and free layers made by sputtering with an industry-standard exchange-bias structure and postdeposition annealing at  $T_a = 400$  °C. The corresponding output voltage swing  $\Delta V$  is over 500 mV, which is five times greater than that of the conventional amorphous Al-O-barrier MTJs. The highest TMR ratio obtained so far is 500% in a pseudospin-valve MTJ annealed at  $T_a = 475$  °C, showing a high potential of the current material system. In addition to this high-output voltage swing, current-induced magnetization switching (CIMS) takes place at the critical current densities ( $J_{co}$ ) on the order of  $10^6$  A/cm<sup>2</sup> in these MgO-barrier MTJs. Furthermore, high antiferromagnetic coupling between the two CoFeB layers in a synthetic ferrimagnetic free layer has been shown to result in a high thermal-stability factor with a reduced  $J_{co}$  compared to single free-layer MTJs. The high TMR ratio enabled by the MgO-barrier MTJs, together with the demonstration of CIMS at a low  $J_{co}$ , allows development of not only scalable magnetoresistive random-access memory with feature sizes below 90 nm but also new memory-in-logic CMOS circuits that can overcome a number of bottlenecks in the current integrated-circuit architecture.

**Index Terms**—CoFeB electrode, magnetoresistive random-access memories (MRAMs), memory-in-logic CMOS circuit, MgO barrier, spintronics, tunnel magnetoresistance (TMR).

Manuscript received November 13, 2006; revised January 22, 2007. This work was supported by the IT-program of Research Revolution 2002 (RR2002): “Development of Universal Low-Power Spin Memory” from the Ministry of Education, Culture, Sports, Science and Technology of Japan. The review of this paper was arranged by Editor H. Morkoc.

S. Ikeda, Y. M. Lee, F. Matsukura, Y. Ohno, and H. Ohno are with the Laboratory for Nanoelectronics and Spintronics, Research Institute of Electrical Communication, Tohoku University, Sendai 980-8577, Japan (e-mail: sikeda@riec.tohoku.ac.jp; ohno@riec.tohoku.ac.jp).

J. Hayakawa is with the Advanced Research Laboratory, Hitachi Ltd., Kokubunji 185-8601, Japan, and also with the Laboratory for Nanoelectronics and Spintronics, Research Institute of Electrical Communication, Tohoku University, Sendai 980-8577, Japan (e-mail: j-hayaka@rd.hitachi.co.jp).

T. Hanyu is with the Laboratory for Brainware Systems, Research Institute of Electrical Communication, Tohoku University, Sendai 980-8577, Japan (e-mail: hanyu@ngc.riec.tohoku.ac.jp).

Color versions of one or more of the figures in this paper are available online at <http://ieeexplore.ieee.org>.

Digital Object Identifier 10.1109/TED.2007.894617

## I. INTRODUCTION

**M**AGNET-BASED nonvolatile memory, such as core memory, was once the choice of main memory of computers [1]. More compact and fast thin magnetic-film memories, developed subsequently that were supposed to be nonvolatile, suffered from creep of domain walls, a slow motion of the boundary of regions having different magnetization directions to reduce the magnetostatic energy, which resulted in loss of information [2]. Soon after, the position enjoyed by the magnetic memories was taken over by more stable and fast semiconductor memories.

Currently, we can define small magnetic elements by lithography, small enough that introduction of domain walls is energetically unfavorable: The domain-wall creep is no longer an issue. The individual magnetic element can also be made virtually nonvolatile; the cutting-edge hard-disk-drive (HDD) technology has proven that magnetic grains of less than 10 nm in diameter can retain its magnetization direction (the coded information) for more than ten years. We can encode these individual magnetic bits electrically and fast, either by external magnetic fields generated by an electrical current (magnetic-field write) [3], [4] or by a spin current produced by a flow of spin-polarized charge current in a magnetic structure (spin-injection write) [5], [6]. The write endurance is virtually unlimited in the former case, according to the knowledge accumulated by the HDD technology. We can read these magnetic bits electrically using magnetic tunnel junctions (MTJs), in which the junction resistance changes with its magnetization state, as shown in Fig. 1. Thus, putting all the existing technologies together in a one MTJ—one transistor (Tr) configuration (we still need a Tr switch to select a bit), one may expect to build a nonvolatile magnetoresistive random-access memory (MRAM) with the bit size of 10 nm, if the Tr can be reduced accordingly.

Fig. 2 shows the MRAM development trend with the International Roadmap for Semiconductors (ITRS) product technology trends for DRAM and Flash for comparison. Here, MRAM stands for those that employ the magnetic-field write, as shown in Fig. 1 [3], [4], [7]–[14], while SPRAM stands for MRAMs that employ the spin-current write [15], [16], which will be described later. Freescale has started shipping 4-Mb MRAM in June 2006 [17]. The trend shows a rapid growth of capacity per chip.

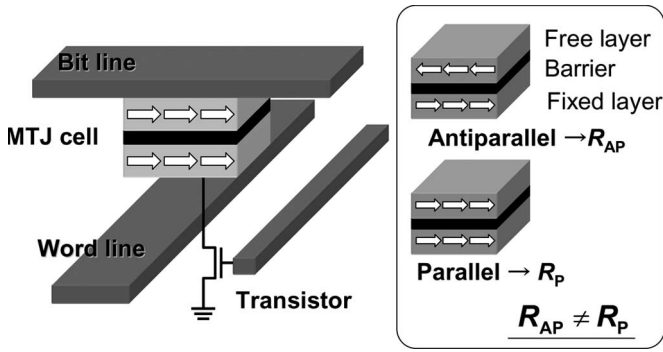


Fig. 1. Schematic diagram of one MTJ-one Tr MRAM cell. The bit-line and the word-line currents together generate a magnetic field high enough to write a cell. For read operation, the bit-line and the (word) line connected to the Tr is used. Spin-injection write (see text) uses current passing through the MTJ; thus, it does not need the word-line. Right figure shows the two states of an MTJ. Free layer is the layer in which information is recorded. Fixed layer is engineered not to change its magnetization direction. A P magnetization configuration between the free layer and the fixed layer results (usually) in a low-resistance ( $R_P$ ) state, while an AP configuration results in a high-resistance ( $R_{AP}$ ) state.

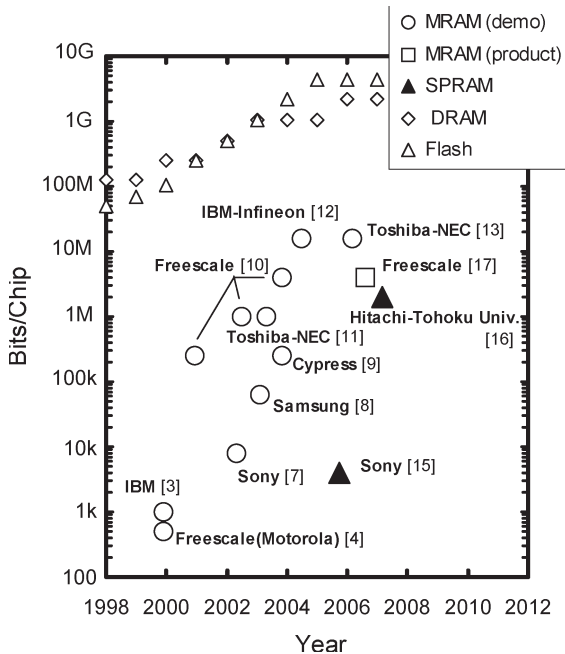


Fig. 2. MRAM development trend.

However, there have been two major obstacles to overcome before this approach becomes truly competitive at a gigabit scale and above. One is the output voltage of an MTJ; the maximum voltage swing produced by a conventional Al-O-barrier MTJ is, at most, 100 mV, not high enough to comfortably integrate them in a gigabit semiconductor circuitry. Another is its scalability. When magnetic fields generated by an electrical current are used to write the direction of a magnet (encoding), the required current increases with the reduction of the size of the magnet (keeping the thickness and magnetization the same). It becomes even more serious for those small magnetic elements designed to show a high thermal stability. The spin-current-write scheme is scalable; as the current needed to switch, a magnet reduces in proportion to the area of an MTJ, because the switching takes place at a certain threshold current

density  $J_C$ . The problem is that the threshold current density has been generally high, on the order of  $10^7$ – $10^8$  A/cm<sup>2</sup>. As we will see in the later sections, the output-voltage barrier is now gone, and the second barrier, the high  $J_C$ , is being reduced considerably, both by the recent development of MgO-barrier MTJs. This new breed of MRAM, called SPRAM, Spin-RAM, or STT-RAM after its write scheme, still needs to go successfully through a number of check-points, which include the reliability of the insulator MgO for high endurance over  $10^{15}$  and the uniformity of the barrier quality over a 300-mm wafer, before it becomes the major and indispensable technology of the semiconductor industry. However, once established, it appears that not only can it offer a fast, scalable, and nonvolatile memory with virtually unlimited endurance, which may not only dramatically reduce the power consumption of a chip, but also open a variety of new directions for integrated circuits. One of the new directions [18] is discussed in the last section of this paper.

## II. MAGNETIC TUNNEL JUNCTIONS

### A. Brief History and Fundamentals of MTJ

An MTJ consists of two ferromagnets separated by a tunnel barrier and changes its resistance depending on the relative orientation of the two magnetization directions of the two magnets due to spin-dependent tunneling involved in the transport between the majority and minority spin states. This resistance change is called tunnel magnetoresistance (TMR), which is defined as  $\Delta R/R = (R_{AP} - R_P)/R_P$ , where  $R_{AP}$  and  $R_P$  are the resistance for antiparallel (AP) and parallel (P) magnetization configurations between the two ferromagnets (see Fig. 1), respectively. In 1975, Julliere discovered TMR in an Fe/Ge/Co junction at low temperature; the TMR ratio was 14% [19]. Maekawa and Gafvert also succeeded in observing the TMR effect again at low temperatures in Ni/NiO/(Ni, Fe, or Co) junctions at the beginning of 1980 [20]. In 1995, the TMR ratios of over 10% at room temperature (RT) were reported in amorphous Al-oxide (Al-O)-barrier MTJs by two groups, Miyazaki and Tezuka at Tohoku University [21] and Moodera and co-workers at MIT [22]. Since these first RT demonstrations, many groups steadily improved the properties of Al-O-barrier MTJs, as shown in Fig. 3. The TMR ratio monotonically increased year by year and reached 70%. This is close to the limit of the TMR ratio expected from the Julliere’s formula [19], in which the TMR ratio is given as  $2P_1P_2/(1 - P_1P_2)$ , where  $P_1$  and  $P_2$  are the spin polarization of the two magnetic layers. When one uses  $P = 52\%$ , measured at 0.2 K for CoFe [23], the TMR ratio becomes slightly over 70%, indicating that Al-O-based MTJs were reaching its limit, according to the simplest model. During the process of increasing the TMR ratio, a number of technologies have also been developed. These include spin-valve structure for stabilization of the AP configuration [24], optimization of ferromagnetic-electrode materials [7], [25]–[27], magnetic-field annealing [28], oxidation method [29], [30], and etching technique.

A typical unit structure of one MTJ-one Tr cell for MRAM is schematically shown in Fig. 1. A modern MTJ has a spin-valve structure (the layer stack, not shown in Fig. 1), which fixes

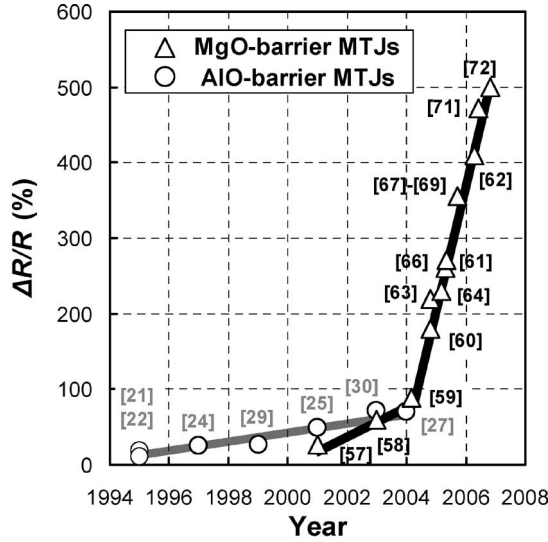


Fig. 3. Development of TMR ratio ( $= \Delta R/R$ ) for MTJs with Al-O and Mg-O tunnel barriers.

the magnetization direction of one of the ferromagnetic layer by the use of exchange interaction between the ferromagnetic layer and the neighboring antiferromagnetic layer; thus, the fixed layer is also called as the reference layer. The other ferromagnetic layer is the layer that changes its magnetization direction according to the input field/current and stores information, hence, called the free layer. Which of the top or bottom layer is fixed depends on the specific design of an MTJ.

### B. Voltage Swing

To make the sensing circuit compatible with the ones used in DRAMs, the voltage swing  $\Delta V$  of an MTJ needs to be  $\Delta V \geq 200$  mV [31], [32]. Otherwise, more elaborate sensing circuitry has to be developed for the readout in the expense of speed. For an MTJ,  $\Delta V$  for readout corresponds to absolute value of TMR ratio  $\times V_P (= |V_{AP} - V_P|)$ , where  $V_{AP}$  and  $V_P$  are the voltage for AP and P magnetization configurations, respectively. The TMR ratio is obtained at a constant bias current of  $i = V_P/R_P (= V_{AP}/R_{AP})$ . As the bias voltage  $V_P$  increases (hereafter, we refer to it as  $V$  for simplicity, which corresponds to the horizontal axis of Fig. 4), the TMR ratio gradually decreases for the reasons not fully established at the moment [33]. As a result,  $\Delta V$  first increases and then gradually decreases as  $V$  increases. This is shown in Fig. 4 for two different Al-O-barrier MTJs. In the case of a CoFe/Al-O/Co MTJ reported in one of the earliest reports [22],  $\Delta V$  was about 10 mV. The  $\Delta V$  for the MTJ with  $\text{Co}_{75}\text{Fe}_{25}/\text{Al-O}/\text{Co}_{75}\text{Fe}_{25}$  spin-valve stacks [25] reached about 100 mV.

### C. Write Current

Reduction of write current is one of the most critical factors to realize a small bit size while keeping the power consumption at a manageable level. Conventional magnetic-field writing is carried out by generating two ‘‘half-select’’ magnetic fields by electrical currents flowing through the word and bit lines, as

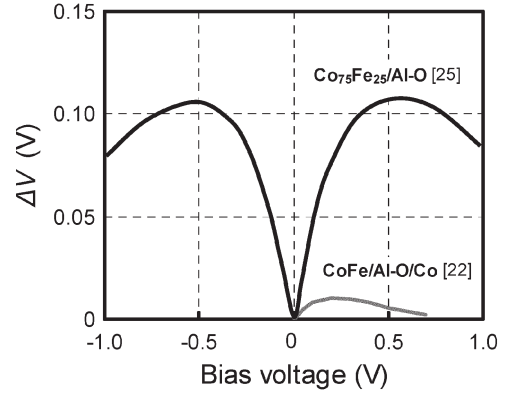


Fig. 4. Bias voltage dependence of the signal voltage  $\Delta V$  for Al-O-barrier MTJs.

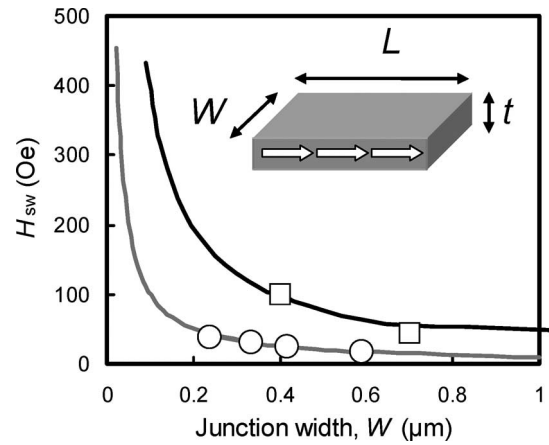


Fig. 5.  $H_{sw}$  as a function of junction width for single  $\text{Co}_{90}\text{Fe}_{10}$  free layers with  $t = 3$  nm and  $k = (L/W) = 2$  (open square) and for  $\text{Ni}_{81.5}\text{Fe}_{18.5}$  free layers with  $t = 4$  nm and  $k = 3$  (open circle).

depicted in Fig. 1. This allows one to access the free layer of the targeted MTJ, while keeping other MTJs intact. We note that considerable effort is required to reduce the distribution of the properties of MTJs to the level low enough for this scheme to be applicable even in the medium-scale integration [10].

The magnetic field ( $H_{sw}$ ) required to switch the free layer can be expressed as

$$H_{sw} = CM_s t/W + H_k \quad (1)$$

where  $t$  and  $W$  are the free-layer thickness and the junction width, respectively,  $M_s$  is the saturation magnetization,  $C$  is a coefficient, and  $H_k$  is the anisotropy field, which includes the effect of crystal magnetic anisotropy and elastic magnetic anisotropy [34], [35]. Because there is not much room for reducing the thickness, (1) indicates that, eventually,  $H_{sw}$  becomes inversely proportional to  $W$ . As shown in Fig. 5,  $H_{sw}$  increases with reduction of  $W$  for 3-nm-thick  $\text{Co}_{90}\text{Fe}_{10}$  magnetic layers with an aspect ratio  $k = L/W = 2$  [35] and for 4-nm-thick  $\text{Ni}_{81.5}\text{Fe}_{18.5}$  magnetic layers with  $k = 3$  [36]. This shows that the write current (power consumption) for switching the free layer increases with increasing the density. The black solid line in Fig. 6 is the calculated value of write current required for conventional magnetic-field writing by using the

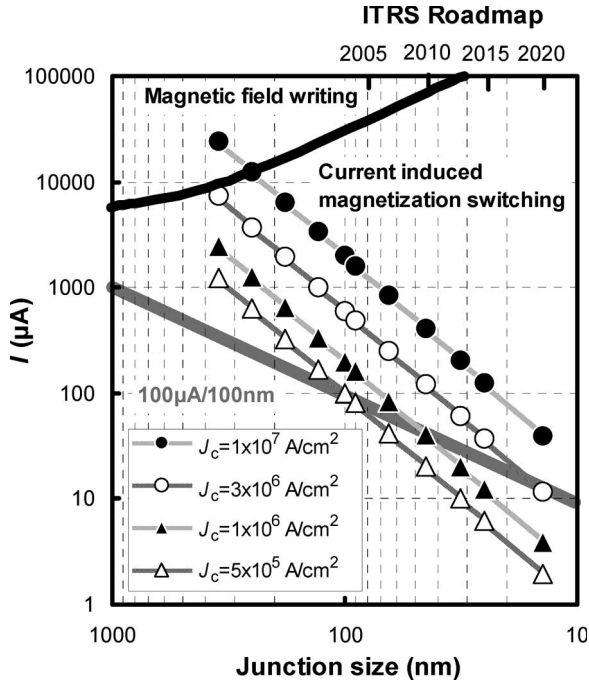


Fig. 6. Current required to observe CIMS as a function of junction size for four different critical current densities. The aspect ratio is assumed to be two. The black thick solid line shows the required current for the magnetic-field write. The gray thick line shows the current that a CMOS with the gate width equal to the junction size can provide (100  $\mu\text{A}/100\text{ nm}$  is assumed). The ITRS technology nodes are also shown. Symbols are guides for the eyes.

$H_{\text{sw}}$  of the  $\text{Ni}_{81.5}\text{Fe}_{18.5}$  layers in Fig. 5. Clearly, this is not scalable and one needs to find a different way of switching.

Theories developed by Slonczewski [5] and Berger [6] indicate that spin-polarized currents exert torque on magnetization and, eventually, may switch the magnetization direction once the current density become sufficiently high. This (spin-polarized) current-induced magnetization switching (CIMS) was first demonstrated on metallic current-perpendicular-to-plane giant magnetoresistance (CPP-GMR) pillars [37], [38] and later on MTJs. CIMS is scalable, because the required absolute current scales with the junction size of the MTJs. Assuming that the critical current density  $J_C$  for CIMS is independent on the junction size, the write current in the range of  $J_C = 5 \times 10^5 - 1 \times 10^7 \text{ A/cm}^2$  is calculated and plotted in Fig. 6, assuming the aspect ratio of two. As shown, in order for this approach to be viable in the 90-nm-technology node and beyond,  $J_C$  must be less than  $10^6 \text{ A/cm}^2$ , as it has to be driven by a MOSFET that can deliver typically 100  $\mu\text{A}/100\text{ nm}$  gate width. This is also shown by a gray solid line in Fig. 6.

Fig. 7 shows the relationship between the TMR ratio ( $= \Delta R/R$ ) and  $J_{C(C0)}$  in the devices for which CIMS were demonstrated ( $J_{C0}$  will be explained later). The Co/Cu/Co CPP-GMR nanopillars show  $J_C$  in the range of mid  $10^6 - 10^8 \text{ A/cm}^2$ , depending on the employed structure, and exhibit magnetoresistance ratio of 0.5%–5% [37]–[43]. The Al-O-barrier MTJs have  $J_C$  similar to CCP-GMR pillars and exhibit TMR ratio of 10%–30% [44]–[47]. The MgO-barrier MTJs, which is the subject of the following section, have been shown to exhibit a high TMR ratio, together with CIMS, in a

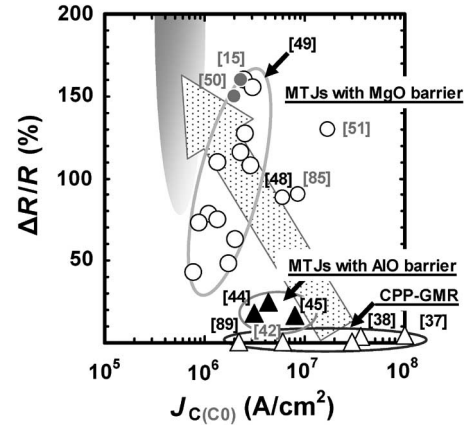


Fig. 7. Relationship between  $\Delta R/R$  and critical current  $J_{C(C0)}$  for the devices for which CIMS were demonstrated. The references, shown in black and gray, correspond to  $J_C$  (measured at RT at current pulswidth ranging from 100 ms to 1 s) and  $J_{C0}$  [ $J_C$  at 1 ns (extrapolated), see text for details], respectively. The shaded area is the region of interest for MRAMs with CIMS writing.

wide range of  $J_C = 8 \times 10^5 - 2 \times 10^7 \text{ A/cm}^2$  [15], [48]–[51]. Note that  $J_C$  depends on the current pulswidth as well. In order for this approach to be competitive, an MTJ has to show a low  $J_C$  on the order of  $10^5 \text{ A/cm}^2$  at reasonably fast pulswidth and the TMR ratio of more than 150%, while not sacrificing the nonvolatility, i.e., the thermal stability. A high thermal-stability factor over 40 ( $E/k_B T$ , where  $E$ ,  $k_B$ , and  $T$  are the energy potential between the two states, the Boltzmann constant, and temperature, respectively) is at least required, which corresponds to retention over ten years on a bit level.

### III. MgO-BARRIER MTJS

#### A. Emergence of MgO-Barrier MTJs

In 2001, Butler *et al.* [52] and Mathon and Umerski [53] pointed out the possibility of realizing high TMR ratios of 100% to even 1000% for fully ordered (001)-oriented Fe/MgO/Fe MTJs by calculations based on the first principle. The TMR ratios of body-centered cubic (bcc) Co (001) and FeCo (001) electrode systems were also predicted to be several times greater than the TMR ratio predicted for the Fe/MgO/Fe system [54]. The giant TMR originates from the fact that the electrons in highly spin-polarized  $\Delta_1$  band in (001) direction of bcc ferromagnetic electrodes can tunnel the MgO (001) barrier more easily than the electrons at other bands ( $\Delta_2$  and  $\Delta_5$ ). They have thus predicted that the effective spin-polarization of bulk bcc Fe, Co, and FeCo in the (001) direction can be dramatically enhanced by spin-filtering of a single-crystal MgO tunnel barrier [52]–[56].

It did not take too long to demonstrate these predictions experimentally [57], [58]. As shown in Fig. 3, the TMR ratio of 88% at RT was reported in 2004 by Yuasa *et al.* [59] for fully epitaxial Fe/MgO-barrier MTJs prepared using molecular beam epitaxy (MBE). This is higher than the highest reported for an Al-O-barrier MTJ (70%) [27]. Subsequent experiments have demonstrated giant TMR ratios of 180% and 410% in fully epitaxial Fe/MgO/Fe and Co/MgO/Co MTJs, respectively

[60]–[62], and of 220% in highly oriented (001) CoFe/MgO/CoFe MTJs [63]. Djavaprawira *et al.* demonstrated the TMR ratio of 230% for sputtered Co<sub>60</sub>Fe<sub>20</sub>B<sub>20</sub>/MgO/Co<sub>60</sub>Fe<sub>20</sub>B<sub>20</sub> MTJs [64], [65], while Hayakawa *et al.* showed 260% for sputtered Co<sub>40</sub>Fe<sub>40</sub>B<sub>20</sub>/MgO/Co<sub>40</sub>Fe<sub>40</sub>B<sub>20</sub> MTJs [66]. The latter developments are particularly notable because they deposited MTJs with a standard spin-valve structure on a thermal oxidized Si wafer using a conventional sputtering system and then annealed the MTJs to obtain a giant TMR ratio, starting from amorphous CoFeB ferromagnetic electrodes. It has also been demonstrated that the spin-valve-type MTJs with Co<sub>40</sub>Fe<sub>40</sub>B<sub>20</sub>/MgO/Co<sub>40</sub>Fe<sub>40</sub>B<sub>20</sub> stack can show very high TMR ratios in a wide-resistance-area product RA, 27% at RA = 0.8 Ω · μm<sup>2</sup> and over 361% from 500 to 10<sup>5</sup> Ω · μm<sup>2</sup> [67]–[69]. Recently, pseudo-spin valve MTJs with CoFeB/MgO/CoFeB stack are shown to exhibit a TMR ratio exceeding 450% [70], [71], reaching 500% at RT, and 1010% at 5 K [72]. These results were realized by direct sputtering of MgO, whereas other methods have been tried such as natural oxidation [73] and plasma oxidation [74]. It is worth noting that high TMR ratio over 100% can be obtained in MgO-based MTJs at temperatures as high as 300 °C [75].

For single-crystal Fe/MgO/Fe MTJs prepared by MBE, ΔV is reported to exceed 500 mV at the positive bias side, whereas it is 300 mV at the negative bias side [60]. This asymmetry is attributed to asymmetric structural defects such as dislocations at the interfaces and the lattice distortions generated during MBE growth. For sputtered Co<sub>60</sub>Fe<sub>20</sub>B<sub>20</sub>/MgO/Co<sub>60</sub>Fe<sub>20</sub>B<sub>20</sub> MTJs, the reported ΔV is about 380 and 330 mV for the negative and positive bias, respectively [64]. By modifying the composition of the electrodes and sputter conditions, the ΔV in CoFeB/MgO/CoFeB MTJs is shown to reach 450–550 mV [66], [71], which is five times greater than that of Al-O-barrier MTJs and is high enough for many applications including high-density MRAMs. Employing a double-barrier structure has also been shown effective in increasing ΔV [76].

### B. TMR Ratio of MgO-Barrier MTJs

To study the relationship between the TMR ratio and the structures as well as the processing conditions of MgO-barrier MTJs, we have fabricated systematically a number of MTJs and compared the TMR ratio, as summarized in Table I.

The MTJ multilayer structure studied here was Si/SiO<sub>2</sub> wafer/Ta(5)/Ru(50)/Ta(5)/NiFe(5)/MnIr(8)/CoFe(2)/Ru(0.8)/fixed layer(3)/MgO(1.5)/free layer(3)/Ta(5)/Ru(15) (in nanometers), deposited using RF magnetron sputtering, where Co<sub>40</sub>Fe<sub>40</sub>B<sub>20</sub>, Co<sub>20</sub>Fe<sub>60</sub>B<sub>20</sub>, Co<sub>50</sub>Fe<sub>50</sub>, and Co<sub>90</sub>Fe<sub>10</sub> alloys (in atomic percent) were used for the fixed and free layers. Here, the bottom CoFe and the fixed layer are strongly coupled by an exchange interaction through Ru, the direction of which is stabilized by the underlying antiferromagnet MnIr. We also studied MTJs with modified structures: 1) Co<sub>50</sub>Fe<sub>50</sub>(2.5)/Co<sub>40</sub>Fe<sub>40</sub>B<sub>20</sub> (3) fixed layer, i.e., without the Ru spacer; 2) Co<sub>40</sub>Fe<sub>40</sub>B<sub>20</sub>(2)/Ni<sub>81</sub>Fe<sub>19</sub>(3) free layer instead of single free layer; and 3) a pseudospin-valve MTJ having a layer stack of Si/SiO<sub>2</sub> wafer/Ta(5)/Ru(20)/Ta(5)/(Co<sub>x</sub>Fe<sub>100-x</sub>)<sub>80</sub>B<sub>20</sub>(4.3)/MgO(*t*<sub>MgO</sub>)/(Co<sub>x</sub>Fe<sub>100-x</sub>)<sub>80</sub>B<sub>20</sub>(4)/

TABLE I  
MAXIMUM TMR RATIO FOR THE MTJs WITH DIFFERENT REFERENCE AND FREE LAYERS ANNEALED AT OPTIMUM TEMPERATURE ( $T_a^{OP}$ ) THAT GIVES THE MAXIMUM TMR RATIO

Fixed layer	Free layer	$T_a^{OP}$ (°C)	TMR ratio (%)
Co <sub>40</sub> Fe <sub>40</sub> B <sub>20</sub>	Co <sub>40</sub> Fe <sub>40</sub> B <sub>20</sub>	400	355
Co <sub>20</sub> Fe <sub>60</sub> B <sub>20</sub>	Co <sub>20</sub> Fe <sub>60</sub> B <sub>20</sub>	400	351
Co <sub>40</sub> Fe <sub>40</sub> B <sub>20</sub>	Co <sub>50</sub> Fe <sub>50</sub>	400	277
Co <sub>40</sub> Fe <sub>40</sub> B <sub>20</sub>	Co <sub>90</sub> Fe <sub>10</sub>	350	131
Co <sub>50</sub> Fe <sub>50</sub>	Co <sub>40</sub> Fe <sub>40</sub> B <sub>20</sub>	325	50
Co <sub>50</sub> Fe <sub>50</sub>	Co <sub>50</sub> Fe <sub>50</sub>	270	12
Co <sub>90</sub> Fe <sub>10</sub>	Co <sub>40</sub> Fe <sub>40</sub> B <sub>20</sub>	300	75
Co <sub>90</sub> Fe <sub>10</sub>	Co <sub>90</sub> Fe <sub>10</sub>	270	53
Co <sub>40</sub> Fe <sub>40</sub> B <sub>20</sub>	Co <sub>40</sub> Fe <sub>40</sub> B <sub>20</sub> /NiFe	300	65
CoFe/Co <sub>40</sub> Fe <sub>40</sub> B <sub>20</sub>	Co <sub>20</sub> Fe <sub>60</sub> B <sub>20</sub>	325	181
(pseudo-spin valve)			
Co <sub>40</sub> Fe <sub>40</sub> B <sub>20</sub>	Co <sub>40</sub> Fe <sub>40</sub> B <sub>20</sub>	450	450
Co <sub>20</sub> Fe <sub>60</sub> B <sub>20</sub>	Co <sub>20</sub> Fe <sub>60</sub> B <sub>20</sub>	475	500

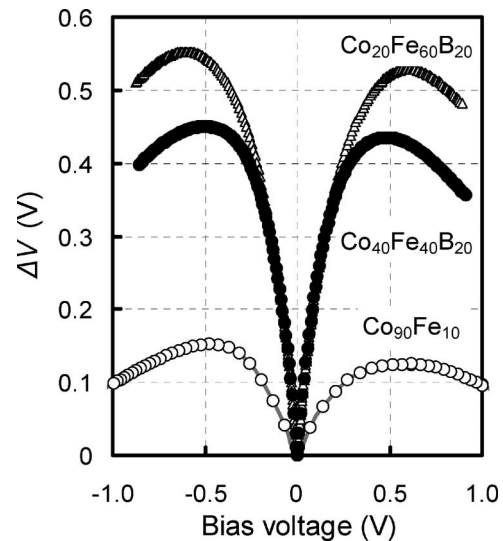


Fig. 8. Bias voltage dependence of the signal voltage ΔV for MgO-barrier MTJs with different ferromagnetic electrodes.

Ta(5)/Ru(10). In CoFeB layer, the composition ratio *x* of Co and Fe was 25 at.% and 75 at.%. The MgO thickness *t*<sub>MgO</sub> was varied from 1.5 to 2.1 nm. All MTJs were microfabricated by photolithography with a junction size of 0.8 × 4.0 μm<sup>2</sup> and were annealed at  $T_a = 250$  °C–500 °C in a vacuum under a field of 4 kOe. TMR ratios were measured using a dc four-probe method at RT in the magnetic-field range of ±1 kOe.

The maximum TMR ratio for the MgO-barrier MTJs with different fixed and free layers annealed at optimum temperature ( $T_a^{OP}$ ), defined as  $T_a$  that results in the highest TMR ratio, are summarized in Table I. The TMR ratio of the MTJ with Co<sub>40</sub>Fe<sub>40</sub>B<sub>20</sub> free and fixed layers increases with increasing  $T_a$  and reaches 355% at  $T_a = 400$  °C. Similar TMR ratio of 351% is observed in the MTJs with Co<sub>20</sub>Fe<sub>60</sub>B<sub>20</sub>. When Co<sub>50</sub>Fe<sub>50</sub> or Co<sub>90</sub>Fe<sub>10</sub> was used for the free and/or fixed layers, no giant TMR ratio was observed, e.g., for the MTJs with Co<sub>40</sub>Fe<sub>40</sub>B<sub>20</sub> free layer and Co<sub>90</sub>Fe<sub>10</sub> fixed layer, the maximum TMR ratio was 75%. Fig. 8 shows the bias voltage dependence of the signal

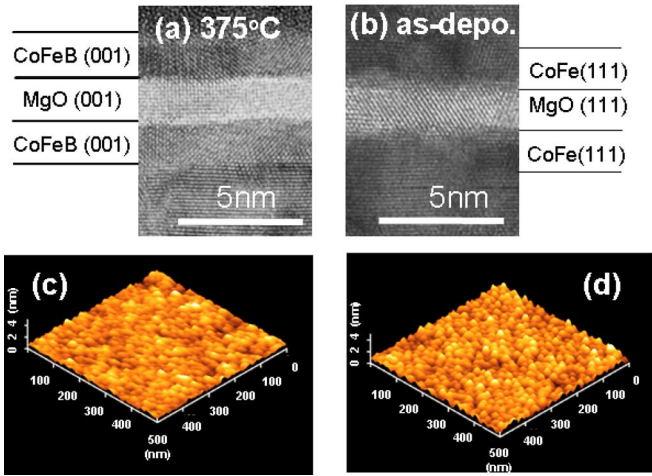


Fig. 9. Cross-sectional TEM images for (a)  $\text{Co}_{40}\text{Fe}_{40}\text{B}_{20}/\text{MgO}/\text{Co}_{40}\text{Fe}_{40}\text{B}_{20}$  after annealing at 375 °C and (b) as-deposited  $\text{Co}_{90}\text{Fe}_{10}/\text{MgO}/\text{Co}_{90}\text{Fe}_{10}$  junctions, and AFM images for  $\text{Ta}(5)/\text{Ru}(50)/\text{Ta}(5)/\text{NiFe}(5)/\text{MnIr}(8)/\text{CoFe}(2)/\text{Ru}(0.8)/X(3)$  samples consisting of  $X =$  (c)  $\text{Co}_{40}\text{Fe}_{40}\text{B}_{20}$  and (d)  $\text{Co}_{90}\text{Fe}_{10}$ .

voltage  $\Delta V$  for MgO-barrier MTJs. The  $\Delta V$  in the MTJ with the  $\text{Co}_{40}\text{Fe}_{40}\text{B}_{20}$  free and fixed layers reached 450 mV. By increasing Fe concentration in the free and fixed layers,  $\Delta V$  increases to 550 mV. MTJ with a  $\text{Co}_{90}\text{Fe}_{10}$  fixed layer shows low  $\Delta V$  of about 150 mV. High  $\Delta V$  is not obtained only by adopting an oriented MgO-barrier but the combination with CoFeB electrodes is thus critical.

To understand the difference of the TMR ratios for the MTJs with different free and fixed layers, the crystalline structures and the surface morphology were measured using cross-sectional high-resolution transmission electron microscopy and atomic force microscope (AFM), respectively. A highly (001)-oriented MgO layer is found to form on the  $\text{Co}_{40}\text{Fe}_{40}\text{B}_{20}$  amorphous fixed layer [64], [66]. Fig. 9(a) reveals that the MgO layer acts as a template for crystallization of initially amorphous  $\text{Co}_{40}\text{Fe}_{40}\text{B}_{20}$  into highly (001)-oriented texture through annealing at high temperatures. When the underlying fixed layer forms an fcc (111)-oriented texture, as shown in Fig. 9(b), for the  $\text{Co}_{90}\text{Fe}_{10}$  fixed layer, the MgO barrier also inherits the texture, resulting in low TMR ratio. The smooth surface of amorphous CoFeBe shown in Fig. 9(c) compared to CoFe [Fig. 9(d)] may also contribute to the (001)-textured MgO formation. Highly oriented (001) MgO barrier/ $\text{Co}_{40}\text{Fe}_{40}\text{B}_{20}$  crystalline electrodes resulted in a high TMR ratio of 355%, whereas MTJs with polycrystalline fcc  $\text{Co}_{90}\text{Fe}_{10}$  fixed layers did not show a high TMR ratio. This can be attributed to the absence of highly (001)-oriented MgO barrier/ferromagnetic electrodes. This supports the theoretical picture [52], [53] in which  $\Delta_1$  bands in bcc (001) electrodes and its selective tunneling in MgO (001) barrier are responsible for the high TMR.

Besides the fixed and free layers that are in direct contact with the MgO barrier, the TMR ratio depends critically on the way the layers are stacked. An MTJ that is composed of  $\text{Co}_{40}\text{Fe}_{40}\text{B}_{20}(2)/\text{Ni}_{81}\text{Fe}_{19}(3)$  free layer showed a low TMR ratio of 65% at  $T_a = 300$  °C, presumably because CoFeB under NiFe does not form a highly oriented (001) texture [77]. An-

other MTJ that is composed of  $\text{Co}_{50}\text{Fe}_{50}(2.5)/\text{Co}_{40}\text{Fe}_{40}\text{B}_{20}(3)$  fixed layer without the Ru spacer exhibited a relatively low TMR ratio of 181% at  $T_a = 325$  °C. This is because the as-deposited CoFe layer forms a bcc (110) texture, which acts as a template for the crystallization of the amorphous CoFeB layer during annealing [72]. A pseudospin-valve MTJ, in which the CoFeB layers are designed to crystallize only from the interface between the MgO barrier, has been shown to exhibit a high TMR of 500% at  $T_a = 475$  °C. This shows that the engineering of the MTJ stack can result in an even higher TMR ratio in exchange-biased MTJs.

### C. CIMS for MgO-Barrier MTJs

In order to fully utilize the potential of CoFeB/MgO/CoFeB MTJs for MRAM and other applications, reduction of the critical current density ( $J_C$ ) for CIMS, while maintaining a high thermal-stability factor well over  $E/k_B T = 40$ , is necessary. While  $J_C$  is proportional to the product of magnetization and thickness (magnetic moment per area) in the free layer, the thermal-stability factor is proportional to the volume of the free layer. If one simply reduces the dimension of an MTJ to accommodate more bits on a given area,  $J_C$  remains constant, but the thermal-stability factor degrades. Synthetic ferrimagnetic (SyF) free layer, consisting of two ferromagnetic layers separated by Ru spacer, is expected to provide a high volume to withstand thermal fluctuations [78]–[81] while keeping the effective magnetic moment per area low. Previous study on CIMS in CPP-GMR nanopillars with SyF free layers reported  $J_C$  lower than that of conventional single free-layer MTJs [82]. We have thus investigated SyF free layers for CoFeB/MgO/CoFeB MTJs.

The MTJ film-layer structure studied was, starting from the substrate side,  $\text{Ta}(5)/\text{Ru}(50)/\text{Ta}(5)/\text{NiFe}(5)/\text{MnIr}(8)/\text{CoFe}(4)/\text{Ru}(0.8)/\text{Co}_{40}\text{Fe}_{40}\text{B}_{20}(5)/\text{MgO}(0.9)/\text{Co}_{40}\text{Fe}_{40}\text{B}_{20}(2)/\text{Ru}(0.7)/\text{Co}_{40}\text{Fe}_{40}\text{B}_{20}(2)/\text{Ta}(5)/\text{Ru}(5)$  (in nanometers). The nanopatterned MTJs with the dimension of  $80 \times 160 \text{ nm}^2$  were annealed at a temperature of 300 °C for 1 h under a magnetic field of 4 kOe. Again, the TMR loops of the MTJs were measured at RT using a four-probe method with a dc bias and a magnetic field of up to 1 kOe. CIMS was evaluated by measuring resistance by 50- $\mu\text{A}$ -step current pulses with the pulse duration ( $\tau_p$ ) varying from 100  $\mu\text{s}$  to 1 s. The current direction is defined as positive when the electrons flow from the top (free) to the bottom (fixed) layer.

Fig. 10(a) and (b) show the  $R$ - $H$  loop and the  $R$  versus pulsed current  $I_p$  with  $\tau_p = 10$  ms under an applied magnetic field of  $-32$  Oe of SyF free MTJ with Ru (0.7) spacer, respectively. The TMR ratio is 90% comparable to the one reported for an MTJ with a 2-nm CoFeB single free layer [49]. The static bias field of  $-32$  Oe was applied along the direction of the fixed CoFeB layer to compensate the offset field arising primarily from the stray fields of the edge of the patterned SyF pinned layer [see Fig. 10(a)]. The average critical current density ( $J_C^{\text{ave}} = (J_C^{\text{P} \rightarrow \text{AP}} - J_C^{\text{AP} \rightarrow \text{P}})/2$ ) to switch the magnetization is  $6.8 \times 10^6 \text{ A/cm}^2$  at  $\tau_p = 10$  ms. Fig. 10(c) shows  $J_C^{\text{ave}}$  as a function of  $\ln(\tau_p/\tau_0)$  for  $\tau_p$  from 100  $\mu\text{s}$  to 1 s. The intrinsic critical current density  $J_{C0}$  and the thermal-stability factor  $E/k_B T$  can be determined from this plot by

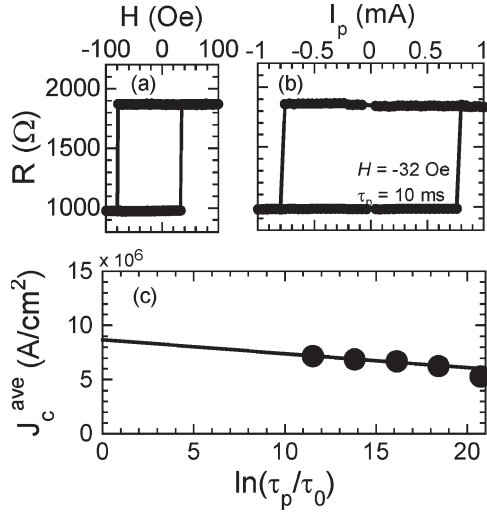


Fig. 10. (a) Resistance ( $R$ ) versus magnetic-field ( $H$ ) loops, (b)  $R$  versus pulsed current ( $I_p$ ) loops at  $\tau_p$  of 10 ms, and (c) the average critical current density  $J_c^{ave}$  ( $(J_c^{P \rightarrow AP} - J_c^{AP \rightarrow P})/2$ ) as functions of  $\ln(\tau_p/\tau_0)$  at RT for an MTJ with a CoFeB(2 nm)/Ru(0.7 nm)/CoFeB(2 nm) SyF free layer.

using the following Slonczewski's model [5] taking into account the thermal-activated nature of the magnetization switching [83], [84]:

$$J_C = J_{C0} \{1 - (k_B T/E) \ln(\tau_p/\tau_0)\} \quad (2)$$

$$J_{C0} = \alpha \gamma e M_s t (H_{ext} \pm H_k \pm H_d) / \mu_B g \quad (3)$$

$$E = M_s V H_k / 2 \quad (4)$$

$$g = P / [2(1 + (P^2 \cos \theta))] \quad (5)$$

where  $\alpha$  is the Gilbert damping coefficient,  $\gamma$  is the gyromagnetic constant,  $e$  is the elementary charge,  $t$  is the thickness of the free layer,  $H_{ext}$  is the external magnetic field,  $H_k$  is the in-plane uniaxial magnetic anisotropy,  $M_s$  is the saturation magnetization of the free layer,  $V$  is the volume of the free layer,  $H_d$  is the out-of-plane magnetic anisotropy induced by the demagnetization field, and  $P$  is the spin polarization.  $\theta$  is zero for the P configuration and  $\pi$  for AP.

Using (2), one can determine  $E/k_B T$  from the slope of Fig. 10(c) to be 67. By extrapolating  $J_C$  to  $\ln(\tau_p/\tau_0) = 0$ , which corresponds to  $\tau_p = 1$  ns (the inverse of ferromagnetic-resonance frequency at zero field), we obtain  $J_{C0}$  of  $8.7 \times 10^6$  A/cm $^2$ . For comparison, we performed the same measurements on MTJs with the 2.2- and 2.5-nm-thick single free layers [i.e., Ta(5)/Ru(50)/Ta(5)/NiFe(5)/MnIr(8)/CoFe(4)/Ru(0.8)/Co $_{40}$ Fe $_{40}$ B $_{20}$ (5)/MgO(0.9)/Co $_{40}$ Fe $_{40}$ B $_{20}$ (2.2, 2.5)/Ta(5)/Ru(5)]. Here,  $J_{C0}$  and  $E/k_B T$  were  $7.6 \times 10^6$  A/cm $^2$  and 27 for the 2.2-nm MTJ, and  $8.4 \times 10^6$  A/cm $^2$  and 36 for the 2.5-nm one, respectively. Having these numbers and using (2) and (4), we can evaluate  $J_{C0}$  and  $E/k_B T$  of an MTJ with a 4-nm-thick single free layer, i.e., of an MTJ that has a single free layer with the CoFeB thickness equal to the sum of the two CoFeB layers in the SyF free layer. This turned out to be  $2.0 \times 10^7$  A/cm $^2$  and 56, respectively. It indicates that employing a SyF free layer increases  $E/k_B T$  as expected,

with reduction of  $J_{C0}$  as compared to the equivalent single free MTJ. The enhanced  $E/k_B T$  is believed to be a result of high coercivity  $H_c$  and strong exchange coupling [85]. The origin of the reduction of  $J_{C0}$  is not fully understood but it may be due to spin-accumulation in the free layer. Two antiferromagnetically coupled CoFeB layers, separated by a nonmagnetic Ru layer whose thickness is much thinner than the spin-diffusion length [86], are known to enhance the spin accumulation at the CoFeB and Ru interface [41], [87]–[89]. Spin accumulation can increase the efficiency of spin-torque acting on the CoFeB free layer and can contribute to the reduction of critical current density.

Although further reduction of  $J_{C0}$  is necessary to realize a current density below  $10^6$  A/cm $^2$ , while maintaining the high thermal stability (i.e., high  $E/k_B T$ ) for MRAM applications, there are a number of strategies one can employ to reduce  $J_{C0}$ . These include 1) dual-spin-filter structure consisting of a free layer sandwiched between the two fixed layers having opposite magnetization configuration, which can enhance the spin accumulation [90], [91], 2) reduction of  $M_s$  and  $\alpha$  by adding other elements to CoFeB or by employing new magnetic materials [92]–[94], 3) employing a controlled pulse shape to realize precharging [95], 4) the use of a nanoaperture structure [96], 5) the use of perpendicular easy-axis [97], and 6) the use of a magnetic-field assisted CIMS [98], [99].

Finally, we note that there are two things to be established before fully exploiting the potential of CIMS for MRAM applications. One is the endurance of MTJs under CIMS. Although  $10^{12}$  has already been shown [15], owing to the relatively low voltage for switching, one needs to demonstrate beyond  $10^{15}$  to call it virtually unlimited. For this, we need to identify and control the failure modes. We also need to understand and control the stochastic nature of switching, particularly at the short pulse duration, where the switching is no longer thermally activated [83], [100], i.e., switching probability is a function of current-pulse magnitude, polarity, and duration [99].

#### IV. MTJ-BASED CMOS LOGIC CIRCUIT

By employing MgO-based MTJs, we have shown that one can achieve a high voltage swing and a scalable switching. The remaining technology issues have been outlined in the last part of the preceding section. Once established, the fast nonvolatile memory with high endurance will not only be a critical ingredient for the reduction of the static power of the advanced very large-scale integration (VLSI) but it will also open new possibilities of overcoming bottlenecks that are present in the current VLSI architecture, one of which is the MTJ-based CMOS logic circuits discussed in this section.

Since an MTJ is a variable two-level resistor, a logic circuit can be built having the logical AND and OR operations between an external input and an internal input stored in an MTJ by series and parallel connection of MTJs and MOS Trs [18]. Arbitrary logic functions with multiple-input variables can be realized by using such an MTJ-based logic-in-memory circuit where storage elements are distributed over a CMOS logic-circuit plane. This approach has been shown to be capable of reducing an effective silicon area and the total leakage

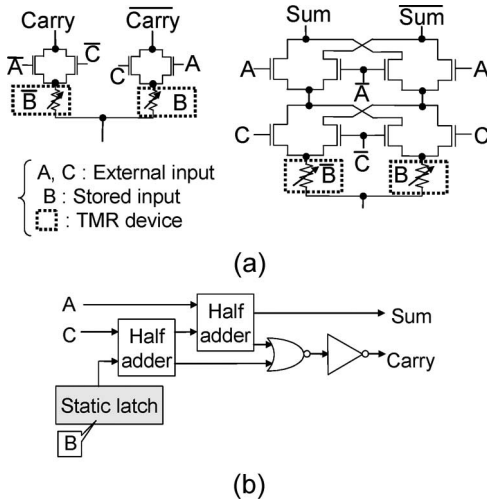


Fig. 11. Full adders. (a) TMR-based full adder. (b) CMOS full adder.

TABLE II  
COMPARISON OF FULL ADDERS

	CMOS	TMR-based
Delay	310ps	310ps
Device counts	40Tr.	24Tr.+2C
Dynamic power	51 $\mu$ W	16 $\mu$ W
Static power	55nW	0.084nW

(0.18 $\mu$ m TMR/CMOS,  $V_{DD}$ =1.8V)

current [101]–[106]. The use of a dynamic current-mode-logic (DyCML) circuit [107] makes it possible to perform a high-speed switching operation in the MTJ-based logic network with less static power dissipation. As a typical example of an MTJ-based logic circuit, an MTJ-based full adder has been designed, as shown in Fig. 11(a), where a stored inputs B and B $\bar$  are directly represented by the resistances of MTJs. Since storage functions are compactly integrated into a logic-circuit network by using MTJs, the total number of Trs in the full adder has been greatly reduced, where the area penalty of the MTJs is not existent because MTJs are stacked on the MOS-Tr plane. Therefore, one can view them as a functional interconnect. Furthermore, the combination of MTJ-based nonvolatile storage elements and DyCML circuit makes it possible to reduce the power dissipation of the designed MTJ-based logic network compared to corresponding CMOS implementation indicated in Fig. 11(b). Table II summarizes the comparison of full adders under a 0.18- $\mu$ m TMR/CMOS technology. In this evaluation, the minimum and maximum resistances of TMR devices are set to be 60 and 90 k $\Omega$ , respectively, i.e., the MR ratio used here is 50%. The total number of Trs, the dynamic power dissipation, and the static power dissipation are reduced to 60%, 31%, and 0.15%, respectively, of the corresponding CMOS counterpart. The static power dissipation becomes zero if the power supply is removed at the standby mode.

The implementation of the MTJ-based CMOS logic-circuit network depends on the MR ratio of MTJs. When the MR ratio becomes sufficiently high, the total Tr counts can further

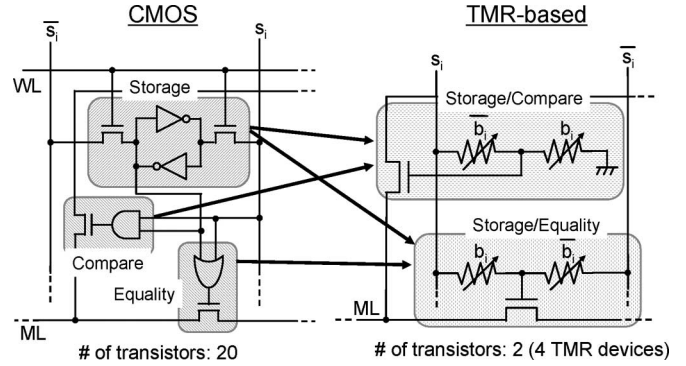


Fig. 12. Design example of CAM cell circuits.

TABLE III  
COMPARISON OF 16-b-WORD CAMS

		CMOS	TMR-based
Delay (ns)		0.69	0.61
Power ( $\mu$ W)	Dynamic	275	193
	Static	16.2	0
# of transistors		5	1

(MR ratio: 1000%)

be reduced, because the output of an MTJ network can be directly used as an input of a MOS-Tr network. For example, Fig. 12 shows a 1-b cell circuit in a fully P content-addressable memory (CAM), where magnitude comparison between an input word and stored words in a CAM is performed in a bit- and word-parallel fashion [18], [108]–[111]. Two kinds of logic functions, 1-b magnitude comparison and equality operations are performed in each CAM cell. Here, the TMR-ratio is assumed to be 1000%. The use of the MTJ-based logic circuit makes a cell circuit compact. Since the leakage-current path is also reduced by using the MTJ-based logic circuit, the static power dissipation can be reduced dramatically. Table III summarizes the comparison of 16-b-word CAMs under a 0.18- $\mu$ m TMR/CMOS technology.

These evaluations show that the use of high TMR MTJs is a promising pathway for realizing a compact hardware and static power saving that allows us to overcome the bottleneck arising from the long interconnects in the current VLSI.

### V. CONCLUSION

We have shown that MgO-barrier-based MTJs show a very high TMR ratio and a low  $J_C$  for CIMS. The TMR ratio in an MTJ with sputtered Co<sub>40</sub>Fe<sub>40</sub>B<sub>20</sub> fixed and free layers using industry-standard exchange-bias structure reached 361% at the postdeposition annealing temperature of  $T_a = 400$   $^{\circ}$ C. The  $\Delta V$  in the MTJ reached 550 mV, which is more than five times than that of MTJs with amorphous Al-O barriers. The key to realize a high TMR ratio is shown to have highly oriented (001)-MgO-barrier/CoFeB crystalline electrodes. The highest TMR ratio, obtained so far in this system, is 500% at  $T_a = 475$   $^{\circ}$ C in a pseudospin-valve MTJ. We found that high antiferromagnetic coupling between the two CoFeB layers in a SyF free layer results in reduced  $J_{C0}$  in CIMS with high

$E/k_B T$  compared to single free-layer MTJs. Memory-in-logic CMOS architecture using MgO-based MTJ is also presented, which may overcome a number of bottlenecks present in the current integrated circuits.

## REFERENCES

- [1] W. H. Rhodes, L. A. Russell, F. E. Sakalay, and R. M. Whalen, "A 0.7-microsecond ferrite core memory," *IBM J. Res. Develop.*, vol. 5, no. 3, pp. 174–182, Jul. 1961.
- [2] W. Anacker, G. F. Bland, P. Pleshko, and P. E. Stuckert, "On the design and performance of a small 60-nsec destructive readout magnetic film memory," *IBM J. Res. Develop.*, vol. 10, no. 1, pp. 41–50, Jan. 1966.
- [3] R. Scheuerlein, W. Gallagher, S. Parkin, A. Lee, S. Ray, R. Robertazzi, and W. Reohr, "A 10 ns read and write non-volatile memory array using a magnetic tunnel junction and FET switch in each cell," in *Proc. IEEE Int. Solid-State Circuits Conf. Dig. Tech. Papers*, Feb. 2000, pp. 128–129.
- [4] M. Durlam, P. Naji, M. DeHerrera, S. Tehrani, G. Kerszykowski, and K. Kyler, "Nonvolatile RAM based on magnetic tunnel junction elements," in *Proc. IEEE Int. Solid-State Circuits Conf. Dig. Tech. Papers*, Feb. 2000, pp. 130–131.
- [5] J. C. Slonczewski, "Current-driven excitation of magnetic multilayers," *J. Magn. Magn. Mater.*, vol. 159, no. 1/2, pp. L1–L7, Jun. 1996.
- [6] L. Berger, "Emission of spin waves by a magnetic multilayer traversed by a current," *Phys. Rev. B, Condens. Matter*, vol. 54, no. 13, pp. 9353–9358, Jan. 1996.
- [7] H. Kano, K. Bessho, Y. Higo, K. Ohba, M. Hashimoto, and M. Hosomi, "MRAM with improved magnetic tunnel junction material," in *Proc. INTERMAG Conf.*, 2002, p. BB-04.
- [8] H. J. Kim, W. C. Jeong, K. H. Koh, G. T. Jeong, J. H. Park, S. Y. Lee, J. H. Oh, I. H. Song, H. S. Jeong, and K. Kim, "A process integration of high-performance 64-kb MRAM," *IEEE Trans. Magn.*, vol. 39, no. 5, pp. 2851–2853, Sep. 2003.
- [9] K. Ounadjela, "MRAM: A new technology for the future," in *Proc. NCCAVS*, Mar. 2004. [Online]. Available: <http://www.avsgroups.org/>
- [10] T. W. Andre, J. J. Nahas, C. K. Subramanian, B. J. Gami, H. S. Lin, A. Omair, and W. L. Martino, Jr., "A 4-Mb 0.18- $\mu\text{m}$  1T1MTJ toggle MRAM with balanced three input sensing scheme and locally mirrored unidirectional write drivers," *IEEE J. Solid-State Circuits*, vol. 40, no. 1, pp. 301–309, Jan. 2005.
- [11] T. Suzuki, Y. Fukumoto, K. Mori, H. Honjo, R. Nebashi, S. Miura, K. Nagahara, S. Saito, H. Numata, K. Tsuji, T. Sugibayashi, H. Hada, N. Ishiwata, Y. Asao, S. Ikegawa, H. Yoda, and S. Tahara, "Toggling cell with four antiferromagnetically coupled ferromagnetic layers for high density MRAM with low switching current," in *VLSI Symp. Tech. Dig.*, 2005, pp. 188–189.
- [12] D. Gogl, C. Arndt, J. C. Barwin, A. Bette, J. DeBrosse, E. Gow, H. Hoenigschmid, S. Lammers, M. Lamorey, Y. Lu, T. Maffitt, K. Maloney, W. Obermaier, A. Sturm, H. Viehmann, D. Willmott, M. Wood, W. J. Gallagher, G. Mueller, and A. R. Sitaram, "A 16-Mb MRAM featuring bootstrapped write drivers," *IEEE J. Solid-State Circuits*, vol. 40, no. 4, pp. 902–907, Apr. 2005.
- [13] Y. Iwata, K. Tsuchida, T. Inaba, Y. Shimizu, R. Takizawa, Y. Ueda, T. Sugibayashi, Y. Asao, T. Kajiyama, K. Hosotani, S. Ikegawa, T. Kai, M. Nakayama, S. Tahara, and H. Yoda, "A 16 Mb MRAM with FORK wiring scheme and burst modes," in *Proc. IEEE Int. Solid-State Circuits Conf. Dig. Tech. Papers*, Feb. 2006, pp. 477–486.
- [14] T. Sakaguchi, H. Choi, S. J. Ahn, T. Sugimura, M. Park, M. Oogane, H. Oh, J. Hayakawa, S. Ikeda, Y. M. Lee, T. Fukushima, T. Miyazaki, H. Ohno, and M. Koyanagi, "Fabrication and evaluation of magnetic tunnel junction with MgO tunneling barrier," *Jpn. J. Appl. Phys.*, vol. 45, no. 4B, pp. 3228–3232, Apr. 2006.
- [15] M. Hosomi, H. Yamagishi, T. Yamamoto, K. Bessho, Y. Higo, K. Yamane, H. Yamada, M. Shoji, H. Hachino, C. Fukumoto, H. Nagao, and H. Kano, "A novel nonvolatile memory with spin torque transfer magnetization switching spin-RAM," in *IEDM Tech. Dig.*, 2005, pp. 459–462.
- [16] T. Kawahara, R. Takemura, K. Miura, J. Hayakawa, S. Ikeda, Y. Lee, R. Sasaki, Y. Goto, K. Ito, T. Meguro, F. Matsukura, H. Takahashi, H. Matsuoka, and H. Ohno, "2 Mb spin-transfer torque RAM (SPRAM) with bit-by-bit bidirectional current write and parallelizing-direction current read," in *Proc. IEEE Int. Solid-State Circuits Conf. Dig. Tech. Papers*, Feb. 2007, pp. 480–481.
- [17] [Online]. Available: <http://www.freescale.com/>
- [18] A. Mochizuki, H. Kimura, M. Ibuki, and T. Hanyu, "TMR-based logic-in-memory circuit for low-power VLSI," *IEICE Trans. Fundam.*, vol. E88-A, no. 6, pp. 1408–1415, Jun. 2004.
- [19] M. Julliere, "Tunneling between ferromagnetic films," *Phys. Lett. A*, vol. 54, no. 3, pp. 225–226, Sep. 1975.
- [20] S. Maekawa and U. Gafvert, "Electron-tunneling between ferromagnetic films," *IEEE Trans. Magn.*, vol. MAG-18, no. 2, pp. 707–708, Mar. 1982.
- [21] T. Miyazaki and N. Tezuka, "Giant magnetic tunneling effect in Fe/Al<sub>2</sub>O<sub>3</sub>/Fe junction," *J. Magn. Magn. Mater.*, vol. 139, no. 3, pp. L231–L234, Jan. 1995.
- [22] J. S. Moodera, L. R. Kinder, T. M. Wong, and R. Meservey, "Large magnetoresistance at room-temperature in ferromagnetic thin-film tunnel-junctions," *Phys. Rev. Lett.*, vol. 74, no. 16, pp. 3273–3276, Apr. 1995.
- [23] D. J. Monsma and S. S. P. Parkin, "Spin polarization of tunneling current from ferromagnet/Al<sub>2</sub>O<sub>3</sub> interfaces using copper-doped aluminum superconducting films," *Appl. Phys. Lett.*, vol. 77, no. 5, pp. 720–722, Jul. 2000.
- [24] Y. Lu, R. A. Altman, A. Marley, S. A. Rishton, P. L. Trouilloud, G. Xiao, W. J. Gallagher, and S. S. P. Parkin, "Shape-anisotropy-controlled magnetoresistive response in magnetic tunnel junctions," *Appl. Phys. Lett.*, vol. 70, no. 19, pp. 2610–2612, May 1997.
- [25] X. F. Han, M. Oogane, H. Kubota, Y. Ando, and T. Miyazaki, "Fabrication of high-magnetoresistance tunnel junctions using Co<sub>75</sub>Fe<sub>25</sub> ferromagnetic electrodes," *Appl. Phys. Lett.*, vol. 77, no. 2, pp. 283–285, Jul. 2000.
- [26] J. H. Yu, H. M. Lee, Y. Ando, and T. Miyazaki, "Electron transport properties in magnetic tunnel junctions with epitaxial NiFe (111) ferromagnetic bottom electrodes," *Appl. Phys. Lett.*, vol. 82, no. 26, pp. 4735–4737, Jun. 2002.
- [27] D. Wang, C. Nordman, J. M. Daughton, Z. Qian, and J. Fink, "70% TMR at room temperature for SDT sandwich junctions with CoFeB as free and reference layers," *IEEE Trans. Magn.*, vol. 40, no. 4, pp. 2269–2271, Jul. 2004.
- [28] M. Sato, H. Kikuchi, and K. Kobayashi, "Effects of interface oxidization in ferromagnetic tunnel junctions," *IEEE Trans. Magn.*, vol. 35, no. 5, pp. 2946–2948, Sep. 1999.
- [29] J. J. Sun, V. Soares, and P. P. Freitas, "Low resistance spin-dependent tunnel junctions deposited with a vacuum break and radio frequency plasma oxidized," *Appl. Phys. Lett.*, vol. 74, no. 3, pp. 448–450, Jan. 1999.
- [30] M. Tsunoda, K. Nishikawa, S. Ogata, and M. Takahashi, "60% magnetoresistance at room temperature in Co-Fe/Al-O/Co-Fe tunnel junctions oxidized with Kr-O<sub>2</sub> plasma," *Appl. Phys. Lett.*, vol. 80, no. 17, pp. 3135–3137, Apr. 2002.
- [31] Y. Nakagome, M. Horiguchi, T. Kawahara, and K. Itoh, "Review and future prospects of low-voltage RAM circuits," *IBM J. Res. Develop.*, vol. 47, no. 5/6, pp. 525–552, Sep.–Nov. 2003.
- [32] W. Mueller, G. Aichmayr, W. Bergner, E. Erben, T. Hecht, C. Kapteyn, A. Kersch, S. Kudelka, F. Lau, J. Luetzen, A. Orth, J. Nuetzel, T. Schloesser, A. Scholz, U. Schroeder, A. Sieck, A. Spitzer, M. Strasser, P.-F. Wang, S. Wege, and R. Weis, "Challenges for the DRAM cell scaling to 40 nm," in *IEDM Tech. Dig.*, 2005, pp. 336–339.
- [33] S. Zhang, P. M. Levy, A. C. Marley, and S. S. P. Parkin, "Quenching of magnetoresistance by hot electrons in magnetic tunnel junctions," *Phys. Rev. Lett.*, vol. 79, no. 19, pp. 3744–3747, Nov. 1997.
- [34] E. Girgis, J. Schelten, J. Shi, J. Janesky, S. Tehrani, and H. Goronkin, "Switching characteristics and magnetization vortices of thin-film cobalt in nanometer-scale patterned arrays," *Appl. Phys. Lett.*, vol. 76, no. 25, pp. 3780–3782, Jun. 2000.
- [35] T. Nozaki, Y. Jiang, H. Sukegawa, N. Tezuka, A. Hirohata, K. Inomata, and S. Sugimoto, "Magnetic switching properties of magnetic tunnel junctions using a synthetic ferrimagnet free layer," *J. Appl. Phys.*, vol. 95, no. 7, pp. 3745–3748, Apr. 2004.
- [36] Y. Fukumoto, H. Numata, K. Suemitsu, K. Nagahara, N. Ohshima, M. Amano, Y. Asao, H. Hada, H. Yoda, and S. Tahara, "Switching-field stabilization against effects of high-temperature annealing in magnetic tunnel junctions using thermally reliable Ni<sub>x</sub>Fe<sub>100-x</sub>/Al-oxide/Ta free layer," *Jpn. J. Appl. Phys.*, vol. 45, no. 5A, pp. 3829–3834, May 2006.
- [37] J. A. Katine, F. J. Albert, R. A. Buhrman, E. B. Myers, and D. C. Ralph, "Current-driven magnetization reversal and spin-wave excitations in Co/Cu/Co pillars," *Phys. Rev. Lett.*, vol. 84, no. 14, pp. 3149–3152, Jul. 2000.
- [38] F. J. Albert, J. A. Katine, R. A. Buhrman, and D. C. Ralph, "Spin-polarized current switching of a Co thin film nanomagnet," *Appl. Phys. Lett.*, vol. 77, no. 23, pp. 3809–3811, Oct. 2000.

- [39] J. Grollier, V. Cros, A. Hamzic, J. M. George, H. Jaffrés, A. Fert, G. Faini, J. B. Youssef, and H. Legall, "Spin-polarized current induced switching in Co/Cu/Co pillars," *Appl. Phys. Lett.*, vol. 78, no. 23, pp. 3663–3665, Apr. 2001.
- [40] J. Z. Sun, D. J. Monsma, D. W. Abraham, M. J. Rooks, and R. H. Koch, "Batch-fabricated spin-injection magnetic switches," *Appl. Phys. Lett.*, vol. 81, no. 12, pp. 2202–2204, Jul. 2002.
- [41] Y. Jiang, S. Abe, T. Ochiai, T. Nozaki, A. Hirohata, N. Tezuka, and K. Inomata, "Effective reduction of critical current for current-induced magnetization switching by a Ru layer insertion in an exchange-biased spin valve," *Phys. Rev. Lett.*, vol. 92, no. 16, p. 167 204, Apr. 2004.
- [42] K. Yagami, A. A. Tulapurkar, A. Fukushima, and Y. Suzuki, "Low-current spin-transfer switching and its thermal durability in a low-saturation-magnetization nanomagnet," *Appl. Phys. Lett.*, vol. 85, no. 23, pp. 5634–5636, Oct. 2004.
- [43] J. Hayakawa, H. Takahashi, K. Ito, M. Fujimori, S. Heike, T. Hashizume, M. Ichimura, S. Ikeda, and H. Ohno, "Current-driven magnetization reversal in exchange-biased spin-valve nanopillars," *J. Appl. Phys.*, vol. 97, no. 11, p. 114 321, Jun. 2005.
- [44] Y. W. Liu, Z. Z. Zhang, P. P. Freitas, and J. L. Martins, "Current-induced magnetization switching in magnetic tunnel junctions," *Appl. Phys. Lett.*, vol. 82, no. 17, pp. 2871–2873, Feb. 2003.
- [45] Y. Huai, F. Albert, P. Nguyen, M. Pakala, and T. Valet, "Observation of spin-transfer switching in deep submicron-sized and low-resistance magnetic tunnel junctions," *Appl. Phys. Lett.*, vol. 84, no. 16, pp. 3118–3120, Feb. 2004.
- [46] G. D. Fuchs, N. C. Emley, I. N. Krivorotov, P. M. Braganca, E. M. Ryan, S. I. Kiselev, J. C. Sankey, D. C. Ralph, R. A. Burman, and J. A. Katine, "Spin-transfer effects in nanoscale magnetic tunnel junctions," *Appl. Phys. Lett.*, vol. 85, no. 7, pp. 1205–1207, Aug. 2004.
- [47] G. D. Fuchs, I. N. Krivorotov, P. M. Braganca, N. C. Emley, A. G. F. Garcia, D. C. Ralph, and R. A. Buhrman, "Adjustable spin torque in magnetic tunnel junctions with two fixed layers," *Appl. Phys. Lett.*, vol. 86, no. 15, p. 152 509, Apr. 2005.
- [48] H. Kubota, A. Fukushima, Y. Ootani, S. Yuasa, K. Ando, H. Maehara, K. Tsunekawa, D. D. Djayaprawira, N. Watanabe, and Y. Suzuki, "Evaluation of spin-transfer switching in CoFeB/MgO/CoFeB magnetic tunnel junctions," *Jpn. J. Appl. Phys.*, vol. 44, no. 40, pp. L1237–L1240, Sep. 2005.
- [49] J. Hayakawa, S. Ikeda, Y. M. Lee, R. Sasaki, T. Meguro, F. Matsukura, H. Takahashi, and H. Ohno, "Current-driven magnetization switching in CoFeB/MgO/CoFeB magnetic tunnel junctions," *Jpn. J. Appl. Phys.*, vol. 44, no. 41, pp. L1267–L1270, Sep. 2005.
- [50] Z. Diao, D. Apalkov, M. Pakala, Y. Ding, A. Panchula, and Y. Huai, "Spin transfer switching and spin polarization in magnetic tunnel junctions with MgO and AlO<sub>x</sub> barriers," *Appl. Phys. Lett.*, vol. 87, no. 23, p. 232 502, Dec. 2005.
- [51] H. Kubota, A. Fukushima, Y. Ootani, S. Yuasa, K. Ando, H. Maehara, K. Tsunekawa, D. D. Djayaprawira, N. Watanabe, and Y. Suzuki, "Dependence of spin-transfer switching current on free layer thickness in Co-Fe-B/MgO/Co-Fe-B magnetic tunnel junctions," *Appl. Phys. Lett.*, vol. 89, no. 3, p. 032 505, Jul. 2006.
- [52] W. H. Butler, X.-G. Zhang, T. C. Schulthess, and J. M. MacLaren, "Spin-dependent tunneling conductance of Fe/MgO/Fe sandwiches," *Phys. Rev. B, Condens. Matter*, vol. 63, no. 5, p. 054 416, Feb. 2001.
- [53] J. Mathon and A. Umerski, "Theory of tunneling magnetoresistance of an epitaxial Fe/MgO/Fe(001) junction," *Phys. Rev. B, Condens. Matter*, vol. 63, no. 22, p. 220 403, Jun. 2001.
- [54] X.-G. Zhang and W. H. Butler, "Large magnetoresistance in bcc Co/MgO/Co and FeCo/MgO/FeCo tunnel junctions," *Phys. Rev. B, Condens. Matter*, vol. 70, no. 17, p. 172 407, Nov. 2004.
- [55] J. D. Burton, S. S. Jaswal, E. Y. Tsymlar, O. N. Mryasov, and O. G. Heinonen, "Atomic and electronic structure of the CoFeB/MgO interface from first principles," *Appl. Phys. Lett.*, vol. 89, no. 14, p. 142 507, Oct. 2006.
- [56] C. Heiliger, P. Zahn, and L. Mertig, "Microscopic origin of magnetoresistance," *Materials Today*, vol. 9, no. 11, pp. 46–54, Nov. 2006.
- [57] M. Bowen, V. Cros, F. Petroff, A. Fert, C. Martinez Boubeta, J. L. Costa-Kramer, J. V. Anguita, A. Cebollada, F. Briones, J. M. de Teresa, L. Morellon, M. R. Ibarra, F. Guell, F. Peiro, and A. Cornet, "Large magnetoresistance in Fe/MgO/FeCo(001) epitaxial tunnel junctions on GaAs(001)," *Appl. Phys. Lett.*, vol. 79, no. 11, pp. 1655–1657, Sep. 2001.
- [58] J. Faure-Vincent, C. Tiusan, E. Jouguet, F. Canet, M. Sajjeddine, C. Bellouard, E. Popova, M. Hehn, F. Montaigne, and A. Schuhl, "High tunnel magnetoresistance in epitaxial Fe/MgO/Fe tunnel junctions," *Appl. Phys. Lett.*, vol. 82, no. 25, pp. 4507–4509, Jun. 2003.
- [59] S. Yuasa, A. Fukushima, T. Nagahama, K. Ando, and Y. Suzuki, "High tunnel magnetoresistance at room temperature in fully epitaxial Fe/MgO/Fe tunnel junctions due to coherent spin-polarized tunneling," *Jpn. J. Appl. Phys.*, vol. 43, no. 4B, pp. L588–L590, Apr. 2004.
- [60] S. Yuasa, T. Nagahama, A. Fukushima, Y. Suzuki, and K. Ando, "Giant room-temperature magnetoresistance in single-crystal Fe/MgO/Fe magnetic tunnel junctions," *Nat. Mater.*, vol. 3, no. 12, pp. 868–871, Dec. 2004.
- [61] S. Yuasa, T. Katayama, T. Nagahama, A. Fukushima, H. Kubota, Y. Suzuki, and K. Ando, "Giant tunneling magnetoresistance in fully epitaxial body-centered-cubic Co/MgO/Fe magnetic tunnel junctions," *Appl. Phys. Lett.*, vol. 87, no. 22, p. 222 508, Nov. 2005.
- [62] S. Yuasa, A. Fukushima, H. Kubota, Y. Suzuki, and K. Ando, "Giant tunneling magnetoresistance up to 410% at room temperature in fully epitaxial Co/MgO/Co magnetic tunnel junctions with bcc Co(001) electrodes," *Appl. Phys. Lett.*, vol. 89, no. 4, p. 042 505, Jul. 2006.
- [63] S. S. P. Parkin, C. Kaiser, A. Panchula, P. M. Rice, B. Hughes, M. Samant, and S.-H. Yang, "Giant tunneling magnetoresistance at room temperature with MgO (100) tunnel barriers," *Nat. Mater.*, vol. 3, no. 12, pp. 662–667, Dec. 2004.
- [64] D. D. Djayaprawira, K. Tsunekawa, M. Nagai, H. Maehara, S. Yamagata, N. Watanabe, S. Yuasa, Y. Suzuki, and K. Ando, "230% room-temperature magnetoresistance in CoFeB/MgO/CoFeB magnetic tunnel junctions," *Appl. Phys. Lett.*, vol. 86, no. 9, p. 092 502, Feb. 2005.
- [65] K. Tsunekawa, D. D. Djayaprawira, M. Nagai, H. Maehara, S. Yamagata, N. Watanabe, S. Yuasa, Y. Suzuki, and K. Ando, "Giant tunneling magnetoresistance effect in low-resistance CoFeB/MgO(001)/CoFeB magnetic tunnel junctions for read-head applications," *Appl. Phys. Lett.*, vol. 87, no. 7, p. 072 503, Aug. 2005.
- [66] J. Hayakawa, S. Ikeda, F. Matsukura, H. Takahashi, and H. Ohno, "Dependence of giant tunnel magnetoresistance of sputtered CoFeB/MgO/CoFeB magnetic tunnel junctions on MgO barrier thickness and annealing temperature," *Jpn. J. Appl. Phys.*, vol. 44, no. 19, pp. L587–L589, Apr. 2005.
- [67] S. Ikeda, J. Hayakawa, Y. M. Lee, R. Sasaki, T. Meguro, F. Matsukura, and H. Ohno, "Dependence of tunnel magnetoresistance in MgO based magnetic tunnel junctions on Ar pressure during MgO sputtering," *Jpn. J. Appl. Phys.*, vol. 44, no. 48, pp. L1442–L1445, Nov. 2005.
- [68] S. Ikeda, J. Hayakawa, Y. M. Lee, T. Tanikawa, F. Matsukura, and H. Ohno, "Tunnel magnetoresistance in MgO-barrier magnetic tunnel junctions with bcc-CoFe(B) and fcc-CoFe free layers," *J. Appl. Phys.*, vol. 99, no. 8, p. 08A907, Apr. 2006.
- [69] Y. M. Lee, J. Hayakawa, S. Ikeda, F. Matsukura, and H. Ohno, "Giant tunnel magnetoresistance and high annealing stability in CoFeB/MgO/CoFeB magnetic tunnel junctions with synthetic pinned layer," *Appl. Phys. Lett.*, vol. 89, no. 4, p. 042 506, Jul. 2006.
- [70] S. Ikeda, J. Hayakawa, Y. M. Lee, F. Matsukura, and H. Ohno, "Dependence of tunnel magnetoresistance on ferromagnetic electrode materials in MgO-barrier magnetic tunnel junctions," *J. Magn. Magn. Mater.* submitted for publication, cond-mat/0608551.
- [71] J. Hayakawa, S. Ikeda, Y. M. Lee, F. Matsukura, and H. Ohno, "Effect of high annealing temperature on giant tunnel magnetoresistance ratio of CoFeB/MgO/CoFeB magnetic tunnel junctions," *Appl. Phys. Lett.*, vol. 89, no. 23, p. 232 510, Dec. 2006.
- [72] Y. M. Lee, J. Hayakawa, S. Ikeda, F. Matsukura, and H. Ohno, unpublished.
- [73] R. Ferreira, P. Wisniewski, P. P. Freitas, J. Langer, B. Ocker, and W. Maass, "Tuning of MgO barrier magnetic tunnel junction bias current for picotesla magnetic field detection," *J. Appl. Phys.*, vol. 99, no. 8, p. 08K706, Apr. 2006.
- [74] T. Dimopoulos, G. Gieres, J. Wecker, N. Wiese, Y. Luo, and K. Samwer, "Large tunnel magnetoresistance with plasma oxidized MgO barrier," *J. Appl. Phys.*, vol. 98, no. 7, p. 073 705, Oct. 2005.
- [75] X. Liu, D. Mazumdar, W. Shen, B. D. Schrag, and G. Xiao, "Thermal stability of magnetic tunneling junctions with MgO barriers for high temperature spintronics," *Appl. Phys. Lett.*, vol. 89, no. 2, p. 023 504, Jul. 2006.
- [76] G. Feng, S. Dijken, and J. M. D. Coey, "Influence of annealing on the bias voltage dependence of tunneling magnetoresistance in MgO double-barrier magnetic tunnel junctions with CoFeB electrodes," *Appl. Phys. Lett.*, vol. 89, no. 16, p. 162 501, Oct. 2006.
- [77] S. Yuasa, Y. Suzuki, T. Katayama, and K. Ando, "Characterization of growth and crystallization processes in CoFeB/MgO/CoFeB magnetic tunnel junction structure by reflective high-energy electron diffraction," *Appl. Phys. Lett.*, vol. 87, no. 24, p. 242 503, Dec. 2005.

- [78] R. C. Sousa, Z. Zhang, and P. P. Freitas, "Synthetic ferrimagnet free layer tunnel junction for magnetic random access memories," *J. Appl. Phys.*, vol. 91, no. 10, pp. 7700–7702, May 2002.
- [79] K. Inomata, T. Nozaki, N. Tezuka, and S. Sugimoto, "Magnetic switching field and giant magnetoresistance effect of multilayers with synthetic antiferromagnet free layers," *Appl. Phys. Lett.*, vol. 81, no. 2, pp. 310–312, Jul. 2002.
- [80] N. Tezuka, N. Koike, K. Inomata, and S. Sugimoto, "Single domain observation for synthetic antiferromagnetically coupled bits with low aspect ratios," *Appl. Phys. Lett.*, vol. 82, no. 4, pp. 604–606, Jan. 2003.
- [81] N. Tezuka, N. Koike, K. Inomata, and S. Sugimoto, "Magnetization reversal and domain structure of antiferromagnetically coupled submicron elements," *J. Appl. Phys.*, vol. 93, no. 10, pp. 7441–7443, May 2003.
- [82] T. Ochiai, Y. Jiang, A. Hirohata, N. Tezuka, S. Sugimoto, and K. Inomata, "Distinctive current-induced magnetization switching in a current-perpendicular-to-plane giant-magnetoresistance nanopillar with a synthetic antiferromagnet free layer," *Appl. Phys. Lett.*, vol. 86, no. 24, p. 242 506, Jun. 2005.
- [83] R. H. Koch, J. A. Katine, and J. Z. Sun, "Time-resolved reversal of spin-transfer switching in a nanomagnet," *Phys. Rev. Lett.*, vol. 92, no. 8, p. 088 302, Feb. 2004.
- [84] D. Lacour, J. A. Katine, N. Smith, M. J. Carey, and J. R. Childress, "Thermal effects on the magnetic-field dependence of spin-transfer-induced magnetization reversal," *Appl. Phys. Lett.*, vol. 85, no. 20, pp. 4681–4683, Nov. 2004.
- [85] J. Hayakawa, S. Ikeda, Y. M. Lee, R. Sasaki, T. Meguro, F. Matsukura, H. Takahashi, and H. Ohno, "Current-induced magnetization switching in MgO barrier based magnetic tunnel junctions with CoFeB/Ru/CoFeB synthetic ferrimagnetic free layer," *Jpn. J. Appl. Phys.*, vol. 45, no. 40, pp. L1057–L1060, Oct. 2006.
- [86] K. Eid, R. Fonck, M. A. Darwish, W. P. Pratt, Jr., and J. Bass, "Current-perpendicular-to-plane-magnetoresistance properties of Ru and Co/Ru interfaces," *J. Appl. Phys.*, vol. 91, no. 10, pp. 8102–8104, May 2002.
- [87] A. Fert, V. Cros, J.-M. Gerorge, J. Grollier, H. Jaffres, A. Hamzic, A. Vaures, G. Faini, J. Ben Youssef, and H. Le Gall, *Magnetization Reversal by Injection and Transfer of Spin: Experiments and Theory*, 2003. cond-mat/0310737.
- [88] A. Shpiro, P. M. Levy, and S. Zhang, "Self-consistent treatment of nonequilibrium spin torques in magnetic multilayers," *Phys. Rev. B, Condens. Matter*, vol. 67, no. 10, p. 104 430, Mar. 2003.
- [89] Y. Jiang, T. Nozaki, S. Abe, T. Ochiai, A. Hirohata, N. Tezuka, and K. Inomata, "Substantial reduction of critical current for magnetization switching in an exchange-biased spin valve," *Nat. Mater.*, vol. 3, no. 6, pp. 361–364, Jun. 2004.
- [90] L. Berger, "Multilayer configuration for experiments of spin precession induced by a dc current," *J. Appl. Phys.*, vol. 93, no. 10, pp. 7693–7695, May 2003.
- [91] Y. Huai, M. Pakala, Z. Diao, and Y. Ding, "Spin transfer switching current reduction in magnetic tunnel junction based dual spin filter structures," *Appl. Phys. Lett.*, vol. 87, no. 22, p. 222 510, Nov. 2005.
- [92] M. Oogane, T. Wakitani, S. Yakata, R. Yilgin, Y. Ando, A. Sakuma, and T. Miyazaki, "Magnetic damping in ferromagnetic thin films," *Jpn. J. Appl. Phys.*, vol. 45, no. 5A, pp. 3889–3891, May 2006.
- [93] Y. Sakuraba, J. Nakata, M. Oogane, Y. Ando, H. Kato, A. Sakuma, T. Miyazaki, and H. Kubota, "Magnetic tunnel junctions using B2-ordered Co<sub>2</sub>MnAl Heusler alloy epitaxial electrode," *Appl. Phys. Lett.*, vol. 88, no. 2, p. 022 503, Jan. 2006.
- [94] Y. Sakuraba, M. Hattori, M. Oogane, Y. Ando, H. Kato, A. Sakuma, T. Miyazaki, and H. Kubota, "Giant tunneling magnetoresistance in Co<sub>2</sub>MnSi/Al–O/Co<sub>2</sub>MnSi magnetic tunnel junctions," *Appl. Phys. Lett.*, vol. 88, no. 19, p. 192 508, May 2006.
- [95] T. Devolder, P. Crozat, J.-V. Kim, C. Chappert, K. Ito, J. A. Katine, and M. J. Carey, "Magnetization switching by spin torque using subnanosecond current pulses assisted by hard axis magnetic fields," *Appl. Phys. Lett.*, vol. 88, no. 15, p. 152 502, Apr. 2006.
- [96] O. Ozatay, N. C. Emley, P. M. Braganca, A. G. F. Garcia, G. D. Fuchs, I. N. Krivorotov, R. A. Buhrman, and D. C. Ralph, "Spin transfer by nonuniform current injection into a nanomagnet," *Appl. Phys. Lett.*, vol. 88, no. 20, p. 202 502, May 2006.
- [97] S. Mangin, D. Ravelosona, J. A. Katine, M. J. Carey, B. D. Terris, and E. E. Fullerton, "Current-induced magnetization reversal in nanopillars with perpendicular anisotropy," *Nat. Mater.*, vol. 5, no. 3, pp. 210–215, Mar. 2006.
- [98] T. Inokuchi, H. Sugiyama, Y. Saito, and K. Inomata, "Current-induced magnetization switching under magnetic field applied along the hard axis in MgO-based magnetic tunnel junctions," *Appl. Phys. Lett.*, vol. 89, no. 10, p. 102 502, Sep. 2006.
- [99] A. A. Tulapurkar, T. Devolder, K. Yagami, P. Crozat, C. Chappert, A. Fukushima, and Y. Suzuki, "Subnanosecond magnetization reversal in magnetic nanopillars by spin angular momentum transfer," *Appl. Phys. Lett.*, vol. 85, no. 22, pp. 5358–5360, Nov. 2004.
- [100] J. Z. Sun, "Spin-current interaction with a monodomain magnetic body: A model study," *Phys. Rev. B, Condens. Matter*, vol. 62, no. 1, pp. 570–578, Jul. 2000.
- [101] W. H. Kautz, "Cellular logic-in-memory arrays," *IEEE Trans. Comput.*, vol. C-18, no. 8, pp. 719–727, Aug. 1969.
- [102] T. Hanyu, K. Teranishi, and M. Kameyama, "Multiple-valued logic-in-memory VLSI based on floating-gate-MOS pass-transistor network," in *Proc. IEEE ISSCC, Dig. Tech. Papers*, Feb. 1998, pp. 194–195.
- [103] T. Hanyu and M. Kameyama, "Multiple-valued logic-in-memory VLSI architecture based on floating-gate-MOS pass-transistor logic," *IEICE Trans. Electron.*, vol. E82-C, no. 9, pp. 1662–1668, 1999.
- [104] T. Hanyu, K. Teranishi, and M. Kameyama, "Multiple-valued logic-in-memory VLSI based on a floating-gate-MOS pass-transistor network," in *Proc. IEEE Int. Solid-State Circuits Conf.*, 1998, vol. 41, pp. 194–195.
- [105] T. Hanyu, H. Kimura, M. Kameyama, Y. Fujimori, T. Nakamura, and H. Takasu, "Ferroelectric-based functional pass-gate for fine-grain pipelined VLSI computation," in *Proc. IEEE Int. Solid-State Circuits Conf., Dig. Tech. Papers*, Feb. 2002, pp. 208–209.
- [106] H. Kimura, T. Hanyu, M. Kameyama, Y. Fujimori, T. Nakamura, and H. Takasu, "Ferroelectric-based functional pass-gate for low-power VLSI," in *Proc. Symp. VLSI Circuits, Dig. Tech. Papers*, Jun. 2002, pp. 196–199.
- [107] M. W. Allam and M. I. Elmasry, "Dynamic current mode logic (DyCML): A new low-power high-performance logic style," *IEEE J. Solid-State Circuits*, vol. 36, no. 3, pp. 550–558, Mar. 2001.
- [108] L. Chisvin and R. J. Duckworth, "Content-addressable and associative memory," *Comput.*, vol. 22, no. 7, pp. 51–63, Jul. 1989.
- [109] T. Hanyu, N. Kanagawa, and M. Kameyama, "Design of a one-transistor-cell multiple-valued CAM," *IEEE J. Solid-State Circuits*, vol. 31, no. 11, pp. 1669–1674, Nov. 1996.
- [110] H. Kimura, T. Hanyu, M. Kameyama, Y. Fujimori, T. Nakamura, and H. Takasu, "Complementary ferroelectric-capacitor logic and its application," in *Proc. IEEE Int. Solid-State Circuits Conf., Dig. Tech. Papers*, Feb. 2003, pp. 160–161.
- [111] H. Kimura, T. Hanyu, M. Kameyama, Y. Fujimori, T. Nakamura, and H. Takasu, "Complementary ferroelectric-capacitor logic for low-power logic-in-memory VLSI," *IEEE J. Solid-State Circuits*, vol. 39, no. 6, pp. 919–926, Jun. 2004.



**Shoji Ikeda** received the B.S., M.S., and D.E. degrees from Muroran Institute of Technology, Muroran, Japan, in 1991, 1993, and 1996, respectively.

He was a Research Associate in the Department of Electrical and Electronic Engineering at the Muroran Institute of Technology from 1996 to 1999. He was with Fujitsu Ltd., Atsugi/Nagano, Japan, from 1999 to 2003. He was with Tohoku University, Sendai, Japan, in 2003, where he is currently an Associate Professor in the Laboratory for Nanoelectronics and

Spintronics, Research Institute of Electrical Communication. His current research interests include magnetic-metal devices with nanostructures and their application.

Dr. Ikeda was the recipient of the Magnetics Society of Japan Distinguished Paper Award in 2003.



**Jun Hayakawa** received the B.E., M.E., and Ph.D. degrees from Nagoya University, Nagoya, Japan, in 1996, 1998, and 1999, respectively, all in materials science and engineering.

He is currently a Senior Researcher in the Advanced Research Laboratory at Hitachi Ltd. His current research interests are focused on nanoscale magnetoresistive devices and their applications.

Dr. Hayakawa was the recipient of the Takei Award from the Magnetics Society of Japan in 1999.



**Young Min Lee** received the B.E. and M.E. degrees in materials science and engineering from the University of Seoul, Seoul, Korea, in 2000 and 2002, respectively, and the Ph.D. degree in applied physics from Tohoku University, Sendai, Japan, in 2005.

He is currently a Researcher in the Research Institute of Electrical Communication, Tohoku University. His current research interests are focused on magnetic devices with nanostructures and their applications.



**Fumihiro Matsukura** received the B.S., M.S., and Ph.D. degrees from Hokkaido University, Sapporo, Japan, in 1988, 1990, and 1993, respectively, all in physics.

He is currently an Associate Professor in the Laboratory for Nanoelectronics and Spintronics, Research Institute of Electrical Communication, Tohoku University, Sendai, Japan. His current research interests are focused on ferromagnetic semiconductors and their applications.



**Yuzo Ohno** received the B.S., M.S., and Ph.D. degrees from the University of Tokyo, Tokyo, Japan, in 1991, 1993, and 1996, respectively, all in electronics engineering.

He is currently an Associate Professor in the Laboratory for Nanoelectronics and Spintronics, Research Institute of Electrical Communication, Tohoku University, Sendai, Japan, where he is currently working on the physics and application of coherent spin dynamics in semiconductor nanostructures.

Dr. Ohno was the recipient of the Sir Martin Wood Prize in 2004 and Japan Society for Promotion of Science Prize in 2005.



**Takahiro Hanyu** (S'87–M'89) received the B.E., M.E., and D.E. degrees from Tohoku University, Sendai, Japan, in 1984, 1986, and 1989, respectively, all in electronic engineering.

He is currently a Professor in the Research Institute of Electrical Communication, Tohoku University, Sendai, Japan. His general research interests include nonvolatile-device-based circuit architecture and its application to next-generation very large-scale integration computing.

Dr. Hanyu was the recipient of the Outstanding Paper Award at IEEE International Symposium on Multiple-Valued Logic in 1986, the Distinctive Contribution Award at IEEE International Symposium on Multiple-Valued Logic in 1988, the Niwa Memorial Award in 1988, the Sakai Memorial Award from the Information Processing Society of Japan in 2000, and the Judge's Special Award at the 9th LSI Design of the Year from the Semiconductor Industry News of Japan in 2002.



**Hideo Ohno** (M'82) received the B.S., M.S., and Ph.D. degrees from the University of Tokyo, Tokyo, Japan, in 1977, 1979, and 1982, respectively.

He spent one year as a visiting graduate student at Cornell University, Ithaca, NY, in 1979. He joined the Faculty of Engineering of Hokkaido University, Sapporo, Japan, in 1982. He was Visiting Scientist at IBM T.J. Watson Research Center, from 1988 to 1990. In 1994, he moved to Tohoku University, Sendai, Japan, as Professor, where he is currently Director in the Laboratory for Nanoelectronics and

Spintronics, Research Institute of Electrical Communication. He is heading an IT program on "Development of Universal Low-Power Spin Memory" funded by MEXT. He is also Research Director in the Semiconductor Spintronics Project, Exploratory Research for Advanced Technology, Japan Science and Technology Agency. His current research interests include physics and applications of spin-related phenomena in semiconductor, as well as in metal-based nanostructures. He has authored and coauthored over 250 journal papers that cover the areas from compound semiconductor materials and devices to non-magnetic semiconductor, ferromagnetic semiconductor, and metal spintronics.

Dr. Ohno was the recipient of the IBM Japan Science Award in 1998, the International Union of Pure and Applied Physics (IUPAP) Magnetism Prize in 2003, Japan Academy Prize in 2005, and the 2005 Agilent Technologies Europhysics Prize. He is currently a member of the editorial board of international journals including *Virtual Journal of Nanoscale Science and Technology*, *Solid State Communications*, and *Semiconductor Science and Technology*.